0026-895X/04/6605-1103–1112$20.00
MOLECULAR PHARMACOLOGY
Copyright © 2004 The American Society for Pharmacology and Experimental Therapeutics
Mol Pharmacol 66:1103–1112, 2004

Vol. 66, No. 5
2774/1178283
Printed in U.S.A.

Mapping of Maurotoxin Binding Sites on hKv1.2, hKv1.3, and hIKCa1 Channels

Violeta Visan, Ziad Fajloun, Jean-Marc Sabatier, and Stephan Grissmer

Department of Applied Physiology, University of Ulm, Ulm, Germany (V.V., S.G.); Laboratoire International Associé d'Ingénierie Biomoléculaire, Centre National de la Recherche Scientifique Unité Mixte Recherche 6560, Marseille, France (Z.F., J.-M.S.)

Received May 17, 2004; accepted July 27, 2004

ABSTRACT

Maurotoxin (MTX) is a potent blocker of human voltage-activated Kv1.2 and intermediate-conductance calcium-activated potassium channels, hIKCa1. Because its blocking affinity on both channels is similar, although the pore region of these channels show only few conserved amino acids, we aimed to characterize the binding sites of MTX in these channels. Investigating the pH_o dependence of MTX block on current through hKv1.2 channels, we concluded that the block is less pH_o-sensitive than for hIKCa1 channels. Using mutant cycle analysis and computer docking, we tried to identify the amino acids through which MTX binds to hKv1.2 and hIKCa1 channels. We report that MTX interacts with hKv1.2 mainly through six strong interactions. Lys^{23} from MTX protrudes into the channel pore interacting with the GYGD motif, whereas Tyr^{32} and Lys^{7} interact with Val^{381}, Asp^{363}, and Glu^{355}, stabilizing the toxin onto the channel pore. Because only Val^{381}, Asp^{363}, and the GYGD motif are conserved in hIKCa1 channels, and the replacement of His^{399} from hKv1.3 channels with a threonine makes this channel MTX-sensitive, we concluded that MTX binds to all three channels through the same amino acids. Glu^{355}, although important, is not essential in MTX recognition. A negatively charged amino acid in this position could better stabilize the toxin-channel interaction and could explain the pH_o sensitivity of MTX block on current through hIKCa1 versus hKv1.2 channels.

It is well recognized that scorpion venoms represent important sources of potassium channel peptide blockers. Interactions between scorpion toxins and potassium channels were investigated in numerous studies and provided insights into the structure and topology of the external pore vestibule of the channels (Hidalgo and MacKinnon, 1995; Aiyar et al., 1996; Rauer et al., 2000; Wrisch and Grissmer, 2000).

Maurotoxin (MTX) is a scorpion toxin isolated recently from the venom of the Tunisian chactoid scorpion *Scorpio maurus palmatus* (Kharrat et al., 1996, 1997; Castle et al., 2003). It belongs to the α-KTX toxins family (Tytgat et al., 1999) (Fig. 1B). It is composed of a 34-amino-acid peptide and has four disulfide bridges with an atypical pattern organization (C1-C5, C2-C6, C3-C4, and C7-C8) compared with other toxins belonging to the same family (C1-C4, C2-C5, C3-C6 for three–disulfide-bridged toxins and C1-C5, C2-C6, C3-C7, and C4-C8 for four–disulfide-bridged toxins) (Kharrat et al., 1996). Despite its different disulfide bridge organization, MTX has the same three-dimensional structure of potassium channels toxin blockers formed by one α-helix and two β-sheets. Moreover, MTX has been reported to block, in *Xenopus laevis* oocytes, IKCa1, Kv1.2, and ShakerB channels with an affinity lower than 10 nM, whereas its affinity for other potassium channels, such as Kv1.1 and Kv1.3, was higher than 50 nM (Kharrat et al., 1996; Avdonin et al., 2000; Lecomte et al., 2000; Castle et al., 2003).

hKv1.2 and hIKCa1 channels are distributed differently in different tissues. hKv1.2 channels are found predominantly in the brain, where they are most likely to be associated with Kv1.1 and Kv1.6 channel subunits accomplishing crucial roles in neuronal signal transmission (Coleman et al., 1999; Monaghan et al., 2001; Dodson et al., 2003). In contrast, hIKCa1 channels are not expressed in brain; however, they have important functions in many peripheral tissues and cells such as erythrocytes, human T lymphocytes, and colon (Grissmer et al., 1993; Ishii et al., 1997; Logsdon et al., 1997; Vandorpe et al., 1998; Ghanshani et al., 2000; Chandy et al., 2001). Because their up-regulation was associated with cell proliferation, hIKCa1 channels were designated as therapeutic targets and, possibly, as markers of physiological and

This work was supported by grants from the Deutsche Forschungsgemeinschaft (GR 848/8-2) and Bundesministerium für Bildung und Forschung (Interdisziplinäres Zentrum für Klinische Forschung B7).

This work was presented in part as a poster (Visan V, Sabatier J-M, and Grissmer S (2004) Is the block of current through voltage-gated Kv1.2 channels by maurotoxin pH_o dependent? *Biophys J* **86**:538a).

Article, publication date, and citation information can be found at http://molpharm.aspetjournals.org.

doi:10.1124/mol.104.002774.

ABBREVIATIONS: MTX, maurotoxin; CTX, charybdotoxin; KTX, kaliotoxin; hKv1.2 and hKv1.3, human voltage-activated potassium channels; hIKCa1, human intermediate-conductance calcium-activated potassium channels; Fmoc, fluorenylmethyloxycarbonyl; wt, wild-type.

pathological cell proliferation (Vandorpe et al., 1998; Khanna et al., 1999; Pena and Rane, 1999; Kohler et al., 2000; Rane, 2000; Wulff et al., 2000; Elliot and Higgins, 2003; Jäger et al., 2004). In our study, we aimed to find all the interactions of MTX with hKv1.2 and hIKCa1 channels and to investigate the possibility of designing future MTX derivatives that would discriminate between these two channels.

To identify the molecular determinants that are responsible for the binding specificity of MTX to hIKCa1 and hKv1.2 channels, we used thermodynamic mutant cycle analysis, as described by Schreiber and Fersht (1995) and Hidalgo and MacKinnon (1995). Thermodynamic mutant cycles assist in studying coupling energies between pairs of amino acids in a protein-protein complex. The dimensionless Ω value indicates the interaction strength of a given channel-toxin pair and can be calculated using toxin half-blocking doses. The change in coupling energy $\Delta\Delta G$ can then be calculated ($\Delta\Delta G = kT \ln \Omega$). The distances between this pair of residues can then be estimated based on the studies of Schreiber and Fersht (1995) and Hidalgo and MacKinnon (1995), assuming that $\Delta\Delta G$ values $\geq$0.5 kcal/mol correspond to an inter-residue distance of $<$5 Å. Because hKv1.2 and hIKCa1 channels show many structural similarities in the pore region with hKv1.3 channels (Fig. 1A), although these channels are not MTX-sensitive, we compared the binding sites of MTX in all three channels. Thus, this study helped us to better understand the mechanism of MTX block on potassium channels and to propose a docking model of MTX into the pore of the hKv1.2 channel.

Materials and Methods

Cells. The COS-7 cell line was maintained in Dulbecco's modified Eagle's medium with Earle's salts (Invitrogen, Paisley, UK), and 10% heat-inactivated fetal calf serum. Cells were kept in a humidified, 10% CO_2 incubator at 37°C.

Solutions. All experiments were carried out at room temperature (21–25°C). Cells were measured in normal mammalian Ringer's solution containing 160 mM NaCl, 4.5 mM KCl, 2 mM $CaCl_2$, 1 mM $MgCl_2$, and 10 mM HEPES, with an osmolarity of 290 to 320 mOsM. The pH_o was adjusted to 7.4 with NaOH. A simple syringe-driven perfusion system was used to exchange the bath solution in the recording chamber. The internal pipette solution used for measuring hKv1.2 and hKv1.3 currents contained 155 mM KF, 2 mM $MgCl_2$, 10 mM EGTA, 10 mM HEPES; the solution used to measure Ca^{2+}-activated potassium currents contained 135 mM potassium aspartate, 8.7 mM $CaCl_2$, 2 mM $MgCl_2$, 10 mM EGTA, and 10 mM HEPES (free $[Ca^{2+}]_i = 10^{-6}$ M). The pH was adjusted to 7.2 with KOH in each solution, and each had osmolarity between 290 and 320 mOsM.

Toxins. MTX and related analogs were chemically produced with the use of the solid-phase technique (Merrifield, 1986) and a peptide synthesizer (model 433A; Applied Biosystems Inc., Foster City, CA). Peptide chains were assembled stepwise on 0.3 mEq of fluorenylmethyloxycarbonyl (Fmoc)-amide resin (0.68 mEq of amino group/g) using 1 mmol of *N*-a-Fmoc amino acid derivatives. The side chain-protecting groups used for trifunctional residues were: trityl for Cys, Asn, and Gln; *tert*-butyl for Ser, Thr, Tyr, and Asp; pentamethylchroman for Arg, and *tert*-butyloxycarbonyl for Lys. The Fmoc-amino acid derivatives were coupled for 20 min as their hydroxybenzotriazole active esters in *N*-methylpyrrolidinone (3.3-fold excess). The peptide resins (~2.5g) were treated for 2.5 h at 25°C with a mixture of trifluoroacetic acid/H_2O/thioanisole/ethanedithiol (88:5:5:2, v/v) in the presence of phenol (2.5 g). The reduced peptides were oxidized/folded at ~2 mM peptide concentration in 200 mM Tris/HCl buffer, pH 8.3 (72 h, 25°C), and purified by reversed-phase high-pressure liquid chromatography (C18 Aquapore, octadecylsilane 20 mm, 250 × 10 mm; PerkinElmer Life and Analytical Sciences, Boston, MA) by means of a 60-min linear gradient of 0.08% (v/v) trifluoroacetic acid/0 to 35% acetonitrile in 0.1% (v/v) trifluoroacetic acid/H_2O at a flow rate of 6 ml/min (l = 230 nm). The peptides were finally characterized for homogeneity (> 99%) and identity by analytical C18 reversed-phase high-pressure liquid chromatography, amino acid analysis, Edman sequencing, and mass spectrometry.

Charybdotoxin (CTX) was obtained from Bachem Biochemica GmbH (Heidelberg, Germany). All lyophilized peptides were kept at −20°C, and the final dilutions were prepared before the measurements in normal Ringer's solution containing 0.1% bovine serum albumin.

Electrophysiology. All the experiments were carried out using the whole-cell recording mode of the patch-clamp technique (Hamill et al., 1981; Rauer and Grissmer, 1996). Electrodes were pulled from glass capillaries (Science Products, Hofheim, Germany) in three stages and fire-polished to resistances measured in the bath of 2.5 to 5 MΩ. Membrane currents were measured with an EPC-9 patch-clamp amplifier (HEKA Elektronik, Lambrecht, Germany) interfaced to a Macintosh computer running the acquisition and analysis software Pulse and PulseFit (HEKA Elektronik). The holding potential in all experiments was −80 mV. Series resistance compensation

Fig. 1. Alignment of channels and toxins. A, amino acid alignment of different potassium channel sequences in the putative pore region. The highlighted positions are important in MTX binding. B, alignment of the amino acid sequences of MTX and CTX.

(80%) was used when currents were bigger than 2 nA. When current exceeded 15 nA, membrane patches were pulled, and measurements were performed in the outside-out configuration. Data analysis was performed in IgorPro 3.1 (WaveMetrics, Lake Oswego, OR), and K_d values were deduced by fitting a modified Hill equation ($X_{toxin}/X_{control} = 1/[1 + ([toxin]/K_d)]$, where X is the peak current (for hKv1.2 and hKv1.3 channels) or the slope of the ramp current [i.e., the conductance measured between −100 and −60 mV (for hIKCa1 channels)] to the normalized data points obtained at more than four different toxin concentrations. This fit indicates that one toxin molecule is sufficient to block the current through the channel. The standard deviations obtained by this fitting routine reflect the uncertainty of the fit. When K_d was deduced from one single concentration the following calculation was used: $K_d = [toxin]/((1/y) - 1)$, where y is the fraction of unblocked peak current or conductance. The value of each toxin concentration was the mean of at least three measurements ± S.D. (where S.D. represents the standard deviations of the calculated K_d values).

Transfection. pcDNA3/Hygro vectors containing the entire coding sequence of hKv1.2 or hIKCa1 or pRCMV vector containing the coding sequence of hKv1.3 (a kind gift from Dr. O. Pongs, University of Hamburg, Germany) were cotransfected together with a green fluorescent protein expressing construct into COS-7 cells using FuGene6 Transfection Reagent (Roche, Mannheim, Germany), and currents were measured 2 to 3 days after transfection.

Mutagenesis. All the hKv1.2 (R354A, E355A, D363A, V381A, V381H, and T383A), and hIKCa1 (D239N) channel mutants were generated with the QuikChange site-directed mutagenesis kit (Stratagene, Heidelberg, Germany), and the mutations were confirmed by sequencing (GATC, Konstanz, Germany). The hKv1.3 (H399T) channel mutant was generated by T. Dreker (University of Ulm, Germany).

Double Mutant Cycle Analysis. This method was extensively used to assess the distances that lie between two interacting amino acids by estimating their strength of interaction. The change in the coupling energy of interaction is given by $\Delta\Delta G = kT \ln \Omega$, where k is Boltzmann's constant, T is the temperature, and Ω is calculated from the K_d values of the wild-type (wt) and mutant channels and toxins, and $\Omega = [K_d$ (wt channel with wt toxin)] × [K_d (mutant channel with mutant toxin)]/([K_d (wt channel with mutant toxin)] × [K_d (mutant channel with wt toxin)]). According to Schreiber and Fersht (1995) and Hidalgo and MacKinnon (1995), if $\Delta\Delta G$ is ≥0.5 kcal/mol, the distance between the two investigated amino acids is smaller than 5 Å.

Docking. For the docking of MTX into the hKv1.2 channel vestibule, we used the crystal structure of the KcsA channel (Doyle et al., 1998) and the KvAP channel (Jiang et al., 2003). The homology model of the hKv1.2 channel was made by replacing the KcsA amino acids with the equivalent amino acids from the hKv1.2 channel sequence. The docking was performed manually by fitting the MTX into the channel pore, similar to the docking of KTX into the mKv1.1 channel vestibule described by Wrisch and Grissmer (2000). The program used for docking was RasMol v2. The orientation of the toxin into the channel was deduced from the changes in affinity of MTX mutants for the wild-type and mutant hKv1.2 channel and mutant cycle analysis.

Results

Our work attempted to characterize the interaction of a pore-blocking toxin, MTX, with hKv1.2 and hIKCa1 channels. Because the block of MTX on current through hIKCa1 channels was reported to be pH_o-dependent, we investigated the pH_o dependence of MTX block on current through hKv1.2 channels. Using mutant cycle analysis, we identified several MTX binding sites for hKv1.2 channels, and we proposed a docking model. In addition, a comparison of the binding sites of MTX for hKv1.2, hIKCa1, and hKv1.3 channels was made.

MTX Blocks Current through Both hKv1.2 and hIKCa1 Channels but Not through Kv1.3 Channels. hKv1.2, hKv1.3, and hIKCa1 channels were expressed in transiently transfected COS-7 cells. The currents through hKv1.2 and hKv1.3 channels were elicited by depolarizing voltage steps of 200 ms from the holding potential −80 mV to +40 mV, whereas hIKCa1 currents were elicited by 1 μM internal calcium and 400-ms voltage ramps from −120 to 0 mV (Fig. 2). To assess the blocking activity of MTX on hKv1.2 and hIKCa1 channels, we applied to the external Ringer's solution 1 nM MTX for hKv1.2 channels and 5 nM MTX for hIKCa1 channels. These concentrations led to a reduction of almost 50% of both the peak current of hKv1.2 channels (Fig. 2A) and the current conductance of hIKCa1 channels (Fig. 2B). The K_d values calculated from concentration dose-responses revealed a half-blocking concentration of 0.7 ± 0.1 nM ($n = 5$) for hKv1.2, and 4.3 ± 0.3 nM ($n = 6$) for hIKCa1, respectively (Fig. 2, A and B, bottom). To block current through hKv1.3 channels, 5 μM MTX was applied to the external Ringer's solution (Fig. 2C). This concentration blocked about 60% of the peak current. Concentration dose-responses allowed us to calculate a K_d of 3.3 ± 0.2 μM ($n = 9$) (Fig. 2C, bottom).

The pH_o Dependence of MTX Block on Current through hKv1.2 Channels. Because MTX block on current through hIKCa1 is pH_o-dependent (Visan et al., 2004), and several reports by now indicate an increase (Deutsch et al., 1991; Perez-Cornejo et al., 1998) or a decrease (Wrisch and Grissmer, 2000) of peptide binding affinities by an increase in pH_o values, we investigated the pH_o dependence of MTX block on current through hKv1.2 channels. We applied 1 nM of MTX to the extracellular Ringer solution, and we deduced the K_d values of MTX block from single concentration calculations as described under *Materials and Methods*. At pH_o 7.4, the K_d value of the MTX block is 0.4 ± 0.2 nM ($n = 5$). Figure 3 shows that the MTX block on current through hKv1.2 channels is not significantly pH_o-dependent at pH_o values of 6.2 (Fig. 3A) and 8.3 (Fig. 3C), where the K_d values are 0.6 ± 0.3 nM ($n = 7$) and 0.6 ± 0.3 nM ($n = 4$), respectively. However, for pH_o values of 9.1, the block of MTX on current through hKv1.2 channels is about 2- to 3-fold weaker [K_d = 1.2 ± 0.5 nM ($n = 4$)] (Fig. 3D).

To test whether the pH_o affects the binding affinities of other pore-blocking peptides, we investigated the pH_o dependence of CTX (Lambert et al., 1990) block on current through hKv1.2 channels. A concentration of 20 nM CTX blocked approximately 50% of the peak current at pH_o 7.4 (Fig. 4B). This concentration was further used to calculate the K_d according to the equation described under *Materials and Methods*. As Fig. 4 shows, CTX blocked the current through hKv1.2 channels with similar potency in pH_o 6.2, 7.4, 8.3, and 9.1; K_d values were 23 ± 2 ($n = 6$), 19 ± 2 ($n = 4$), 24 ± 6 ($n = 6$), and 25 ± 4 nM ($n = 6$), respectively. These results would confirm the theory that higher pH_o values might slightly change the three-dimensional structure of MTX and thus decrease its blocking affinity for hIKCa1 and hKv1.2 channels (see *Discussion*).

Important Amino Acids for MTX-hKv1.2 Channel Interaction. To identify the important amino acids in MTX-hKv1.2 interaction, five candidate amino acids from hKv1.2

channel were selected (Fig. 1A, highlighted amino acids) and mutated to alanine (or, in the case of Val, to histidine as well, for a total of six mutants): R354A, E355A, D363A, V381A, V381H, and T383A. The selection of these amino acids was made based on computer simulations (Fu et al., 2002) or previous reports of the importance in MTX or other peptide toxins binding of the amino acids situated in equivalent positions in other potassium channels. Thus, it has been reported that position 381 from hKv1.2 channels is important in ShakerB channels for MTX binding (Thr^{499}) (Avdonin et al., 2000), whereas in mKv1.3 channels, the corresponding amino acid (His^{404}) is important in the binding of tetraethylammonium (Bretschneider et al., 1999), CTX (Rauer et al., 2000), or KTX (Aiyar et al., 1996). Likewise, position 363 from hKv1.2 channels has been reported as an important position in hIKCa1 channels (Asp^{239}) for CTX binding (Rauer et al., 2000), whereas the corresponding amino acid of position 355 from hKv1.2 channels has been shown to have a small influence in KTX binding to Kv1.1 channels (Glu^{353}) (Wrisch and Grissmer, 2000). For MTX were selected six peripheral amino acids (S6A, K7A, Y10A, R14Q, K23A, and Y32A) that have been shown to influence MTX binding (Castle et al., 2003). The blocking affinities of MTX or mutant MTX for wild-type or modified hKv1.2 channels is represented in Fig. 5A. The only mutation in the channel that drastically modified MTX binding affinity is hKv1.2_V381H.

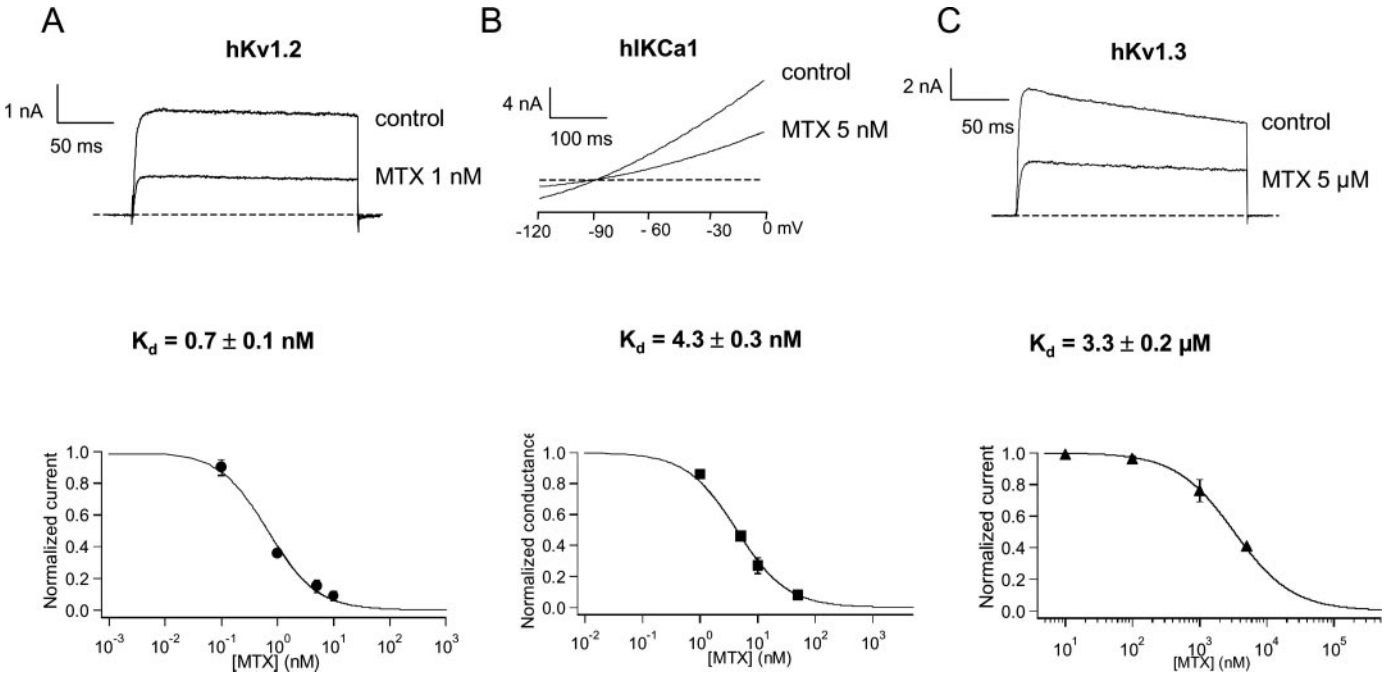

Fig. 2. MTX is a potent blocker of hKv1.2 and hIKCa1 channels, but not of hKv1.3 channels. A, potassium currents through hKv1.2 channel in the absence and the presence of 1 nM MTX. Currents were elicited using an use-dependent pulse protocol, consisting of 10 depolarizing voltage steps of 200 ms, from the membrane potential, −80 to +40 mV, repeated every second. The dose-response curve revealed a K_d of 0.7 ± 0.1 nM (n = 5). B, potassium currents through hIKCa1 channel in the absence and the presence of 5 nM MTX. Currents were elicited using 400-ms voltage ramps from −120 to 0 mV, repeated each 15 s. The dose-response curve revealed a K_d of 4.3 ± 0.3 nM (n = 4). C, potassium currents through hKv1.3 channel in the absence and the presence of 5 μM MTX. Currents were elicited using voltage steps of 200 ms, from the membrane potential, − 80 to +40 mV, repeated every 40 s. The dose-response curve revealed a K_d of 3.3 ± 0.2 μM (n = 9).

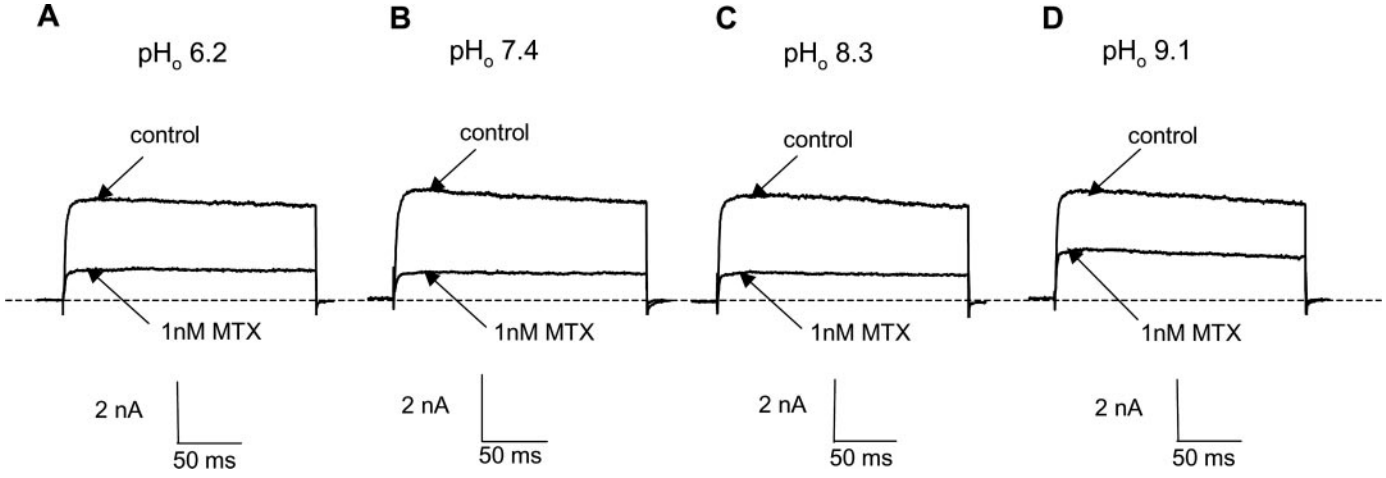

Fig. 3. pH_o-dependent block of extracellularly applied MTX on currents through hKv1.2 channels. Currents were elicited by 10 voltage steps of 200 ms from −80 to +40 mV, every second. Currents were measured in normal Ringer's solution with pH_o 6.2 (A), 7.4 (B), 8.3 (C), and 9.1 (D), before (control) and after application of 1 nM MTX.

The replacement of Val[381] with a histidine [the amino acid that corresponds to His[399] from hKv1.3 channel or Tyr[82] from KcsA channel (Fig. 1A)] changed MTX blocking affinity more than 350-fold, from 0.7 ± 0.1 nM (n = 5) to 255 ± 55 nM (n = 4). For the other channel mutations, MTX blocking affinity was not affected (hKv1.2_R354A, hKv1.2_D363A, and hKv1.2_T383A) or was affected with a difference of <10-fold (hKv1.2_E355A and hKv1.2_V381A). MTX mutations had a greater effect on the binding affinities of the peptides, with a decrease of more than 1000-fold for MTX_K23A and MTX_Y32A, and ~100-fold for MTX_R14Q and MTX_K7A, results that are in agreement with previous studies (Castle et al., 2003). The inferred K_d values (Fig. 5A) were further used to perform mutant cycle analysis and to calculate the change in coupling energy ($\Delta\Delta G$) between different amino acid pairs (Fig. 5*B*). The change in coupling energy allowed us to estimate the distance that lies between certain toxin-channel amino acids. If $\Delta\Delta G$ is ≥0.5 kcal/mol, the distance between

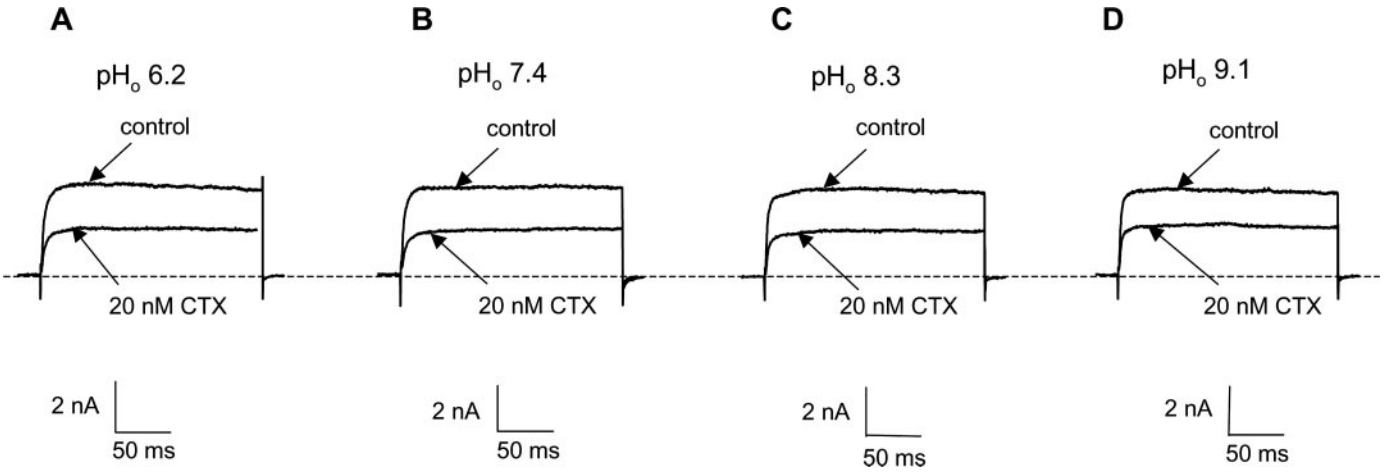

Fig. 4. pH$_o$-dependent block of extracellularly applied CTX on currents through hKv1.2 channels. Currents were elicited by 10 voltage steps of 200 ms from −80 to +40 mV, every second. Currents were measured in normal Ringer's solution with pH$_o$ 6.2 (A), 7.4 (B), 8.3 (C), and 9.1 (D), before (control) and after application of 20 nM CTX.

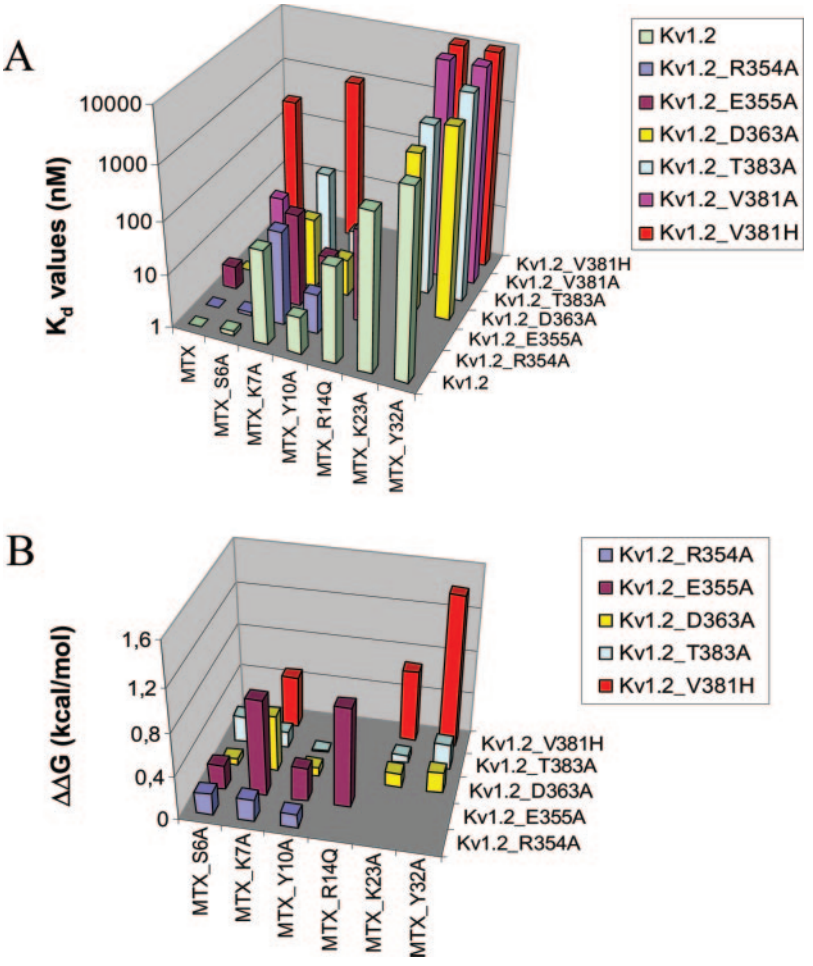

Fig. 5. K_d values and calculated changes in coupling energies ($\Delta\Delta G$) for wild-type and mutant MTX and hKv1.2 channels. A, K_d values calculated using dose-response curves or single concentration (when K_d values were larger than 100 nM) as described under *Materials and Methods*. B, $\Delta\Delta G$ calculated (as described under *Materials and Methods*) using the K_d values of the wild-type and mutant MTX and hKv1.2 channels.

two amino acids is less than 5 Å (Schreiber and Fersht, 1995). The mutation to alanine of the amino acids Ser^{6} and Tyr^{10} from MTX and Arg^{345} and Thr^{383} from hKv1.2 channels apparently did not make a difference in MTX-hKv1.2 interaction, because the calculated change in coupling energies between them and different amino acids from the channel/toxin were smaller than 0.5 kcal/mol (Fig. 5B). Two possibilities could account for this. Either the substitution to alanine of these amino acids does not bring a drastic change in coupling energy because alanine has been replaced by amino acids with equally favorable interactions as they occur in the case of the wild-type channels/wild-type toxin or these amino acids do not participate in the interaction. In the following, we focused on the other amino acid residues in which the change in coupling energy was more than 0.49 kcal/mol.

Shown in Fig. 6, A and B, is an example of a significant change in the binding affinity of a mutant toxin for the hKv1.2 channel. The substitution of K7A makes the toxin almost 100 times less potent for hKv1.2 channels; the K_d value decreased from 0.7 ± 0.1 nM (n = 5) (for the wild-type MTX) to 59 ± 4 nM (n = 4) (for the MTX_K7A mutant). Mutant cycle analysis shows a change in coupling energy of 0.52 kcal/mol between Lys^{7} and Asp^{363} and 0.9 kcal/mol between Lys^{7} and Glu^{355} (Fig. 6C), suggesting that Lys^{7} is situated near these two amino acids, the distance that separates them being less than 5 Å.

A key role in MTX binding seems to have Val^{381} from the hKv1.2 channel. The calculated ΔΔG values indicate that Val^{381} is very near (<5 Å) Lys^{7}, Lys^{23}, and Tyr^{32} from MTX, because their changes in coupling energies are bigger than 0.5 kcal/mol (Fig. 6C).

MTX Binding Sites for hIKCa1 Channels. To test whether MTX has the same binding sites for hIKCa1 as for hKv1.2 channels, we mutated the Asp^{239} to Asn. This amino acid is highly conserved among the Kv1 potassium channel family and corresponds to Asp^{363} from hKv1.2 channels and His^{399} from hKv1.3 channels (Fig. 1A). Figure 7, A and B, shows the loss in blocking affinity of MTX_K7A mutant for hIKCa1 channel [32 ± 3 nM (n = 4) versus 4.3 ± 0.3 nM (n = 6) for the wild-type toxin]. Mutant cycle analysis reveals a change in coupling energy between Asp^{239} and Lys^{7} of 0.49 kcal/mol (Fig. 7C), which would indicate a distance between these two amino acids of ~5 Å. These results, together with the drastic loss in affinity of two of the MTX mutants (MTX_K23A and MTX_Y32A) for hIKCa1 channels (Castle et al., 2003), and the computer simulations made by Fu et al. (2002), indicate at least three common binding sites of MTX for both hKv1.2 and hIKCa1 channels.

MTX Binding Sites for hKv1.3 Channels. Because MTX blocks hKv1.3 with very low affinity [K_d = 3.3 ± 0.2 μM (n = 9)] (Fig. 8A), we mutated one amino acid that corresponds to a key binding amino acid in hKv1.2, and we investigated the MTX blocking activity of this mutant channel. His^{399} from hKv1.3 corresponds to Val^{381} from hKv1.2, Thr^{451} from ShakerB channels, and Tyr^{82} from KcsA channels (Fig. 1A). Because ShakerB channels are also sensitive to MTX, we

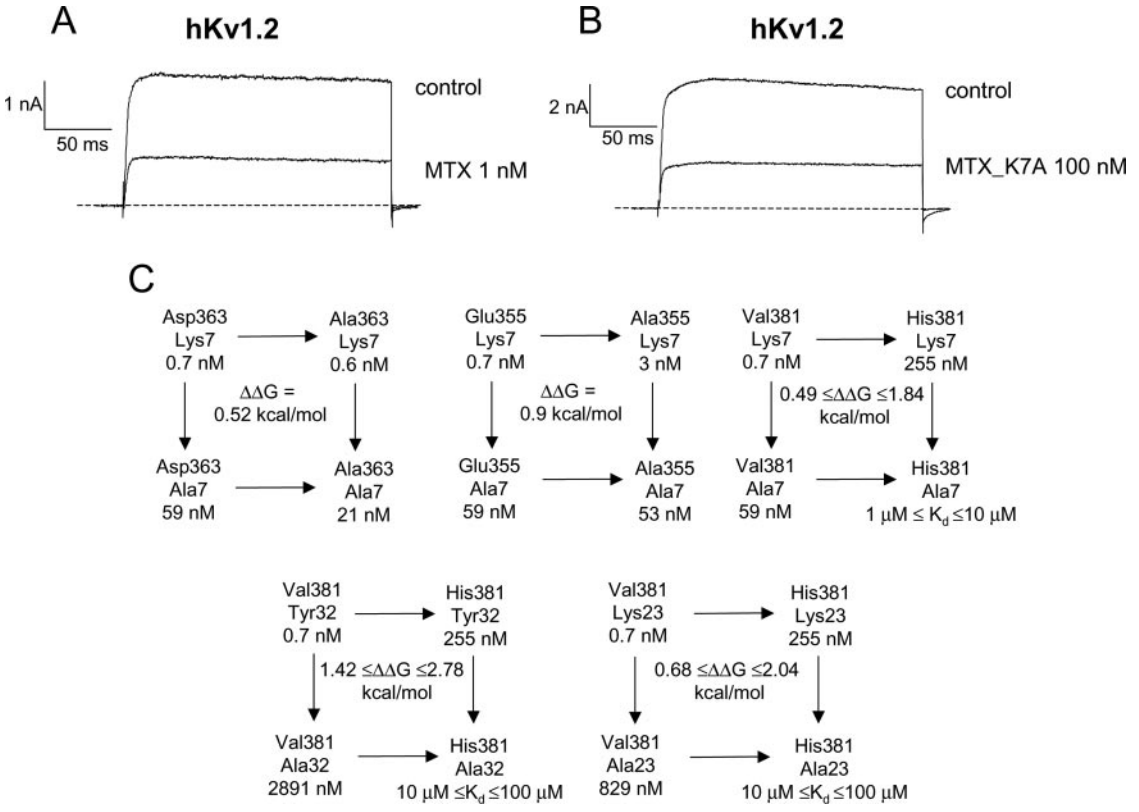

Fig. 6. Comparative block of wild-type (A) and mutant (B) MTX on currents through hKv1.2 channels. The original current traces through hKv1.2 channels represented in the figures were measured in transiently transfected COS-7 cells and elicited by 10 depolarizing voltage steps of 200 ms, from the membrane potential, −80 to +40 mV, every second. C, thermodynamic mutant cycle for the most strongly coupled pairs of residues involved in the binding of MTX to the external vestibule of hKv1.2 channels. The K_d values were calculated using dose-response or single concentration (when K_d values were bigger than 100 nM) as described under *Materials and Methods*. The changes in coupling energies (ΔΔG) for wild-type and mutant MTX and hKv1.2 channels were calculated using the K_d values of the wild-type and mutant MTX and hKv1.2 channels (see *Materials and Methods*).

mutated the His[399] from hKv1.3 channel to threonine. We were surprised to find that the MTX blocking affinity for hKv1.3_H399T was increased by ~10,000-fold; the K_d value was identical to the one with which MTX blocks hKv1.2: 0.6 ± 0.1 nM (n = 7) (Fig. 8B). Because 1 μM MTX_Y32A is inactive on current on hKv1.3 channel, we calculated the change in the coupling energy of this interaction, assuming that K_d was between 100 μM and 1 mM. With these approximations, mutant cycle analysis shows a strong change in the coupling energy (3.21 kcal/mol if we assume that the K_d of hKv1.3 and MTX_Y32A is 100 μM, and 1.84 kcal/mol if we assume that K_d is 1 mM) between Thr[399] and Tyr[32], suggesting that these amino acids come very near each other and that this position is crucial for channel recognition and interaction (Fig. 8C).

Discussion

Our work aimed to characterize the interaction of MTX with hKv1.2 and hIKCa1 channels. We report that basic pH_o values do influence the block of MTX on current through hKv1.2 channels a little, whereas acidic pH_o does not interfere with MTX blocking activity at all. Several binding sites were identified, and a docking model was proposed. In addition, common binding sites of MTX for hKv1.2, hKv1.3 and hIKCa1 channels were found.

Several reports have shown that the pH_o can influence the blocking affinity of pore-blocking peptides (Deutsch et al., 1991; Perez-Cornejo et al., 1998; Bretschneider et al., 1999; Thompson and Begenisich, 2000; Wrisch and Grissmer, 2000). Moreover, we reported that MTX blocks hIKCa1 channels in a pH_o-dependent manner, having lower binding affinities in Ringer solution with pH_o 6.2, 8.3, and 9.1 compared with measurements done at pH_o 7.4 (Visan et al., 2004). We reported that the pH_o dependence at low pH_o was caused by the presence of a histidine in the pore region of hIKCa1 channels (position 236) (Fig. 1A), which probably becomes protonated and thus might repel a positively charged amino acid from the toxin. However, in Ringer solution with high

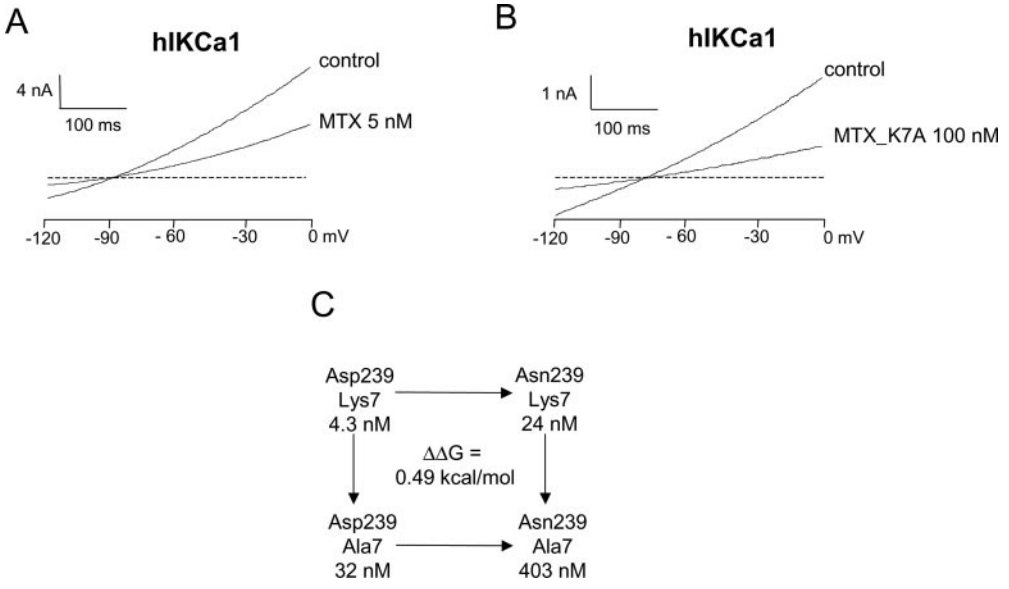

Fig. 7. Comparative block of wild-type (A) and mutant (B) MTX on currents through hIKCa1 channels. The original current traces through hIKCa1 channels represented in the figures were measured in transiently transfected COS-7 cells and elicited by 1 μM $[Ca^{2+}]_i$ and 400 ms voltage ramps, from −120 to 0 mV, every 15 s. C, thermodynamic mutant cycle performed for MTX_Lys[7] and hIKCa1_Asp[239]. The K_d values were calculated using dose-response or single concentration (when K_d values were bigger than 100 nM) as described under *Materials and Methods*. The changes in coupling energy ($\Delta\Delta G$) for wild-type and mutant MTX and hIKCa1 channels were calculated using the K_d values of the wild-type and mutant MTX and hIKCa1 channels (see *Materials and Methods*).

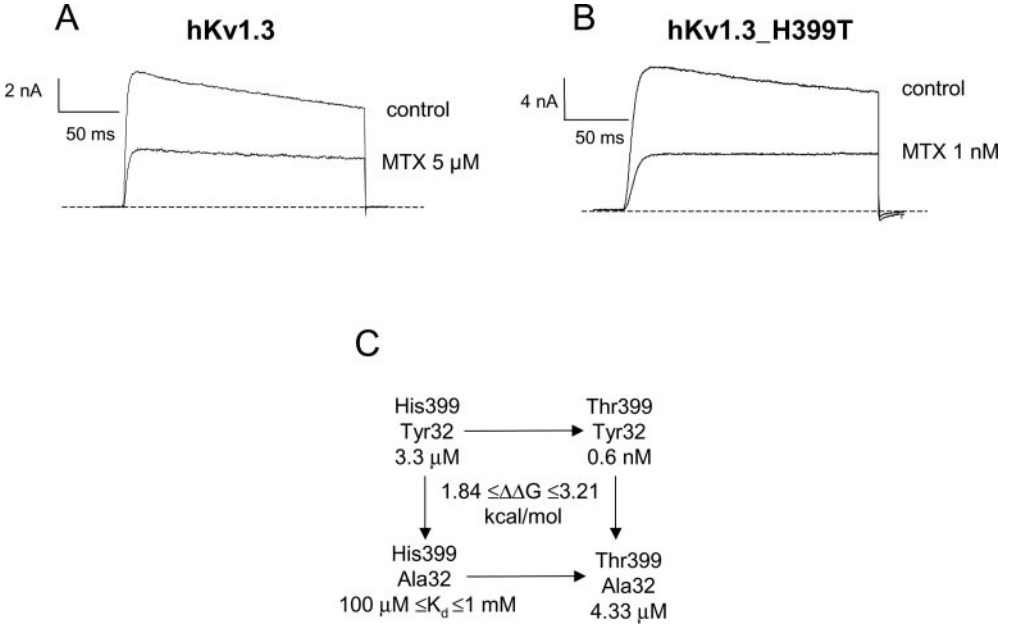

Fig. 8. Comparative block of MTX on currents through wild-type (A) and mutant (B) hKv1.3 channels. The original current traces through hKv1.3 channels represented in the figures were measured in transiently transfected COS-7 cells and elicited by 200-ms depolarizing voltage steps, from the membrane potential −80 to +40 mV, every 40 s. C, thermodynamic mutant cycle performed for MTX_Tyr[32] and hKv1.3_His[399]. The K_d values were calculated using dose-response or single concentrations (when K_d values were greater than 100 nM) as described under *Materials and Methods*. The changes in coupling energy ($\Delta\Delta G$) for wild-type and mutant MTX and hKv1.3 channels was calculated using the K_d values of the wild-type and mutant MTX and hKv1.3 channels (see *Materials and Methods*).

pH_o values, the pH_o dependence of the block can be explained not through the protonation of an amino acid but rather through a slight conformational change of the toxin that might make it fit worse in the channels pore and/or a partial loss of the exposed positively charged amino acids from the toxin that might interact with the negative charges from the channel (Kharrat et al., 1996). This theory is confirmed by our present study, because the block of MTX on current through hKv1.2 channels is not pH_o-dependent at pH_o 6.2 and shows a very weak pH_o dependence only at pH_o 9.1. It seems that the lack of a protonable amino acid in the pore region of hKv1.2 (Fig. 1A) channels makes the MTX block insensitive to pH_o changes toward acidic values. However, the conformational changes of the toxin at higher pH_o values confirmed by circular dichroism spectroscopy analysis (Kharrat et al., 1996) are also sensed by the hKv1.2 channel, although to a lesser extent than by hIKCa1 channel, leading to a weaker block of the modified MTX. Moreover, the comparative study made with CTX demonstrated that only MTX block is affected by the pH_o changes; CTX block on current through both hKv1.2 and hIKCa1 channels was not pH_o-dependent.

Studies of toxin-channel interaction (Hidalgo and MacKinnon, 1995; Aiyar et al., 1996; Rauer et al., 2000; Wrisch and Grissmer, 2000) indicate that all the investigated peptide toxins have two to three amino acids that are essential for binding: one lysine that protrudes into the channel pore and one or two other amino acids that anchor the toxin and stabilize the interaction (usually arginines or lysines). Using the thermodynamic mutant cycle analysis and an approximate toxin docking into hKv1.2 channel, we identified six amino acid pairs that seem to be involved in channel recognition and/or the stabilization of MTX-hKv1.2 channel interaction. The docking was made using the distances estimated through the mutant cycle analysis. They indicated the orientation of the toxin in the channel and allowed us to perform an approximate fitting of MTX into the hKv1.2 channel vestibule. A homology model of KcsA and KvAP channels was used, with the presumption that the external vestibules of these channels and those of the family of mammalian Kv channels are structurally similar. The drastic loss in affinity of MTX_K23A mutant for both hKv1.2 (Fig. 5A) and hIKCa1 channels (Castle et al., 2003), the proximity of Lys^{23} to Val^{381} revealed by the mutant cycle analysis, and the computer simulations made by Fu et al. (2002), indicate that Lys^{23} (green) is the pore-protruding amino acid that interacts with the GYGD motif of the potassium channels and corresponds to Lys^{27} in agitoxin 2, CTX, and KTX (Hidalgo and MacKinnon, 1995; Aiyar et al., 1996; Rauer et al., 2000) (Fig. 9). The mutant cycle analysis also confirms that Tyr^{32} (violet) is very near Val^{381} from hKv1.2 channel (orange) (His^{399} in hKv1.3 channel); they probably form, together with Lys^{23}, the "functional dyad" of MTX. Our data also indicate a strong change in coupling energy between Lys^{7} (red) and Asp^{363} (yellow), and Glu^{355} (blue) from one channel subunit, and Val^{381} (orange), probably from the next channel subunit, suggesting a distance of <5 Å between Lys^{7} and these amino acids (Fig. 9). These interactions should tilt the MTX and bring the Lys^{27} (green) near the Glu^{355} (blue) and/or Asp^{363} (yellow) from the next subunit (Fig. 9).

Using mutant cycle analysis, we also found a strong change in coupling energy (0.92 kcal/mol) between Arg^{14} and Glu^{355} (Fig. 5B). However, we must keep in mind that the point mutation of Arg^{14} to glutamine changes the disulfide bridge organization of MTX toward the Pi1/HsTx1 pattern, which leads to a slight modification of the three-dimensional structure of the peptide (Fajloun et al., 2000). Because Lys^{27} seems to be important in toxin-channel interaction (Fu et al., 2002), it could be that a change in the three-dimensional structure of MTX_R14Q [like the one described by Fajloun et al. (2000) for MTX_K15Q] might place this amino acid in a different position and thus might alter an important electrostatic contact. If the mutant cycle analysis is reliable when there are no conformational changes of the peptide and the channel, we will consider the 5-Å distance between Arg^{14} and Glu^{355} an incorrect estimation.

Comparing the amino acid sequence of hKv1.2 and hIKCa1 channels, we observe that three of the amino acids involved in MTX binding are conserved in both channels: the Tyr^{377} and Asp^{379} from the GYGD motif and the Asp^{363} (Fig. 1A).

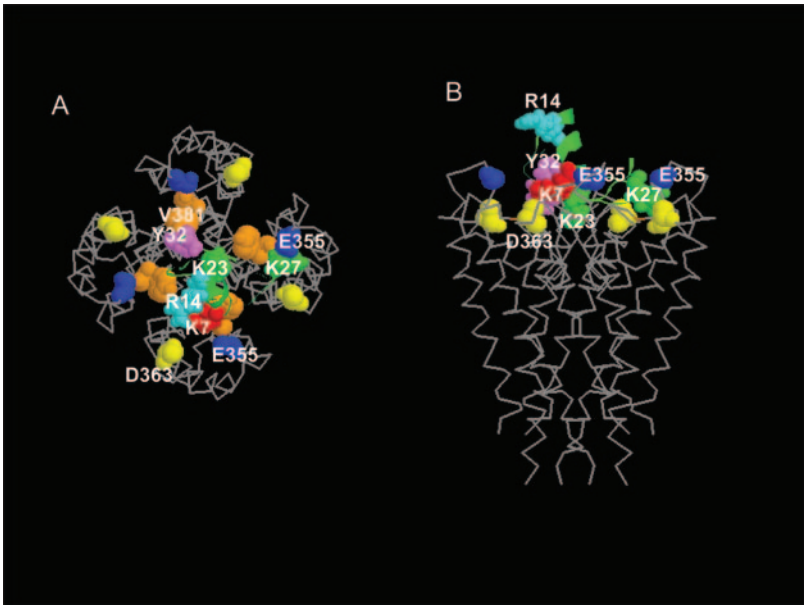

Fig. 9. Docking of MTX into a homology model of the hKv1.2 channel. The docking configuration is shown as top (A) and side (B) views. The homology structure of the hKv1.2 channel is based on the KcsA and KvAP crystal structure. The channel backbone is represented in gray, whereas MTX is shown as green ribbons. Interacting channel amino acids are represented in blue (Glu^{355}), yellow (Asp^{363}), and orange (Val^{381}) as space-filled sections, whereas their interacting toxin partners are represented in cyan (Arg^{14}), red (Lys^{7}), green (Lys^{23}), and violet (Tyr^{32}) sections. The figure was made using RasMol ver. 2.

Val^{381} from the hKv1.2 channel corresponds to His^{399} in the hKv1.3 channel; because this histidine makes the hKv1.3 channel insensitive to MTX block, we presume that this position has an essential role for MTX recognition. This position seems to be a hydrophobic amino acid, such as valine or threonine, to make the channel MTX-sensitive.

One might speculate about the role of Glu^{355} in hKv1.2 channels in the toxin-channel interaction. Because MTX blocks both hKv1.2 and hKv1.3_H399T channels with the same potency, and this amino acid is not conserved in the two channels, being replaced by an uncharged amino acid in hKv1.3_H399T channels, one could argue that this position in hKv1.2 channel might either not be important in MTX binding or might uncover a negative interaction that is the same in both channel mutants. The mutation in the toxin might obviate this negative interaction, resulting in an apparent coupling energy.

Although the role of Glu^{355} from hKv1.2 channels in MTX-hKv1.2 channel interaction might not be clear, it is still possible that this position is important in the fine pharmacological discriminations between hKv1.2 and hIKCa1 channels and could possibly explain why slight modifications of MTX structure (induced, for example, by Ringer solution with basic pH_o) can be better sensed by hIKCa1 than by hKv1.2 channels, causing higher loss in affinity in the first case. This Glu^{355} might stabilize MTX-hKv1.2 channel interaction, and make it less sensitive to structural alterations of toxin and/or channel (Visan et al., 2004).

Conclusions

Our findings suggest similarities in MTX binding to hKv1.2, hIKCa1, and hKv1.3 channels. We report that MTX occludes the pore region of these channels by establishing strong interactions between Lys^{23} and the GYGD motif, Tyr^{32}-Val^{381}, Lys^{7}-Asp^{363}, Lys^{7}-Val^{381} from hKv1.2 channel or the correspondent amino acids from the other channels. The other interactions that Lys^{7} and/or Lys^{27} makes with Glu^{355} are not essential, because the replacement of Glu^{355} with a neutral amino acid weakly affects toxin-channel binding affinity. However, the amino acid situated in this position might be responsible for a better stabilization of the interaction and might explain the pH_o sensitivity of MTX block on current through hIKCa1 versus hKv1.2 channels. Our work describing the amino acids involved in complex formation localizes the regions of binding and, by the calculated energies of interaction, makes estimations on the distances that lie between the interacting amino acids of MTX and different potassium channels. Through the topological information of these toxin-channel interactions that our study brings, these data might be helpful for future drug design studies.

References

Aiyar J, Rizzi JP, Gutman GA, and Chandy KG (1996) The signature sequence of voltage-gated potassium channels projects into the external vestibule. *J Biol Chem* **271:**31013–31016.

Avdonin V, Nolan B, Sabatier J-M, De Waard M, and Hoshi T (2000) Mechanisms of maurotoxin action on Shaker potassium channels. *Biophys J* **79:**776–787.

Bretschneider F, Wrisch A, Lehmann-Horn F, and Grissmer S (1999) External tetraethylammonium as a molecular caliper for sensing the shape of the outer vestibule of potassium channels. *Biophys J* **76:**2351–2360.

Castle NA, London DO, Creech C, Fajloun Z, Stocker JW, and Sabatier J-M (2003) Maurotoxin: a potent inhibitor of intermediate conductance Ca^{2+}-activated potassium channels. *Mol Pharmacol* **63:**409–418.

Chandy KG, Cahalan MD, Pennington M, Norton RS, Wulff H, and Gutman GA (2001) Potassium channels in T lymphocytes: toxins to therapeutic immunosuppresants. *Toxicon* **39:**1269–1276.

Coleman SK, Newcombe J, Pryke J, and Dolly JO (1999) Subunit composition of Kv1 channels in human CNS. *J Neurochem* **73:**849–858.

Deutsch C, Price M, Lee S, King VF, and Garcia ML (1991) Characterization of high affinity binding sites for charybdotoxin in human T lymphocytes. Evidence for association with the voltage-gated K^+ channel. *J Biol Chem* **266:**3668–3674.

Dodson PD, Billups B, Rusznak Z, Szucs G, Barker MC, and Forsythe ID (2003) Presynaptic rat Kv1.2 channels suppress synaptic terminal hyperexcitability following action potential invasion. *J Physiol* **550:**27–33.

Doyle DA, Morais Cabral J, Pfuetzner RA, Kuo A, Gulbis JM, Cohen SL, Chait BT, and MacKinnon R (1998) The structure of the potassium channel: molecular basis of K^+ conduction and selectivity. *Science (Wash DC)* **280:**69–77.

Elliot JI and Higgins CF (2003) IKCa1 activity is required for cell shrinkage, phosphatidylserine translocation and death in T lymphocytes apoptosis. *EMBO Rep* **4:**189–194.

Fajloun Z, Mosbah A, Carlier E, Mansuelle P, Sandoz G, Fathallah M, Luccio E, Devaux C, Rochat H, Darbon C, et al. (2000) Maurotoxin versus Pi1/HsTx1 scorpion toxins. Toward new insights in the understanding of their distinct disulfide bridge patterns. *J Biol Chem* **275:**39394–39402.

Fu W, Cui M, Briggs JM, Huang X, Xiong B, Zhang Y, Luo X, Shen J, Ji R, and Chen K (2002) Brownian dynamics simulations of the recognition of the scorpion toxin maurotoxin with the voltage-gated potassium ion channels. *Biophy J* **83:**2370–2385.

Ghanshani S, Wulff H, Miller MJ, Rohm H, Neben A, Gutman GA, Cahalan MD, and Chandy KG (2000) Up-regulation of the IKCa1 potassium channel during T-cell activation. Molecular mechanism and functional consequences. *J Biol Chem* **275:**37137–37149.

Grissmer S, Nguyen AN, and Cahalan MD (1993) Calcium-activated potassium channels in resting and activated human T lymphocytes. Expression levels, calcium dependence, ion selectivity and pharmacology. *J Gen Physiol* **102:**601–630.

Hamill OP, Marty A, Neher E, Sakmann B, and Sigworth FJ (1981) Improved patch-clamp techniques for high-resolution current recording from cells and cell-free membrane patches. *Pfleug Arch Eur J Physiol* **391:**85–100.

Hidalgo P and MacKinnon R (1995) Revealing the architecture of a K^+ channel pore through mutant cycles with a peptide inhibitor. *Science (Wash DC)* **268:**307–310.

Ishii TM, Silvia C, Hirschberg B, Bond CT, Adelman JP, and Maylie J (1997) A human intermediate conductance calcium-activated potassium channel. *Proc Natl Acad Sci USA* **94:**11651–11656.

Jäger H, Dreker T, Buck A, Giehl K, Gress T, and Grissmer S (2004) Blockage of intermediate-conductance Ca^{2+}-activated K^+ channels inhibit human pancreatic cancer cell growth in vitro. *Mol Pharmacol* **65:**630–638.

Jiang Y, Lee A, Chen J, Ruta V, Cadene M, Chait BT, and MacKinnon R (2003) X-ray structure of a voltage-dependent K^+ channel. *Nature (Lond)* **423:**33–41.

Khanna R, Chang MC, Joiner WJ, Kaczmarek LK, and Schlichter LC (1999) hSK4/hIK1, a calmodulin-binding KCa channel in human T lymphocytes. Roles in proliferation and volume regulation. *J Biol Chem* **274:**14838–14849.

Kharrat R, Mabrouk K, Crest M, Darbon H, Oughideni R, Martin-Eauclaire M-F, Jaquet G, El Ayeb M, Van Rietschoten J, Rochat H, et al. (1996) Chemical synthesis and characterization of maurotoxin, a short scorpion toxin with four disulfide bridges that acts on K^+ channels. *Eur J Biochem* **242:**491–498.

Kharrat R, Mansuelle P, Sampieri F, Crest M, Oughideni R, Van Rietschoten J, Martin-Eauclaire MF, Rochat H, and El Ayeb M (1997) Maurotoxin, a four disulfide bridge toxin from *Scorpio maurus* venom: purification, structure and action on potassium channels. *FEBS Lett* **406:**284–290.

Kohler R, Degenhardt C, Kuhn M, Runkel N, Paul M, and Hoyer J (2000) Expression and function of endothelial Ca^{2+}-activated K^+ channels in human mesenteric artery: a single-cell reverse transcriptase-polymerase chain reaction and electrophysiological study in situ. *Circ Res* **87:**496–503.

Lambert P, Kuroda H, Chino N, Watanabe TX, Kimura T, and Sakakibara S (1990) Solution synthesis of charybdotoxin (ChTX), a K^+ channel blocker. *Biochem Biophys Res Commun* **170:**684–690.

Lecomte C, Ben Khalifa R, Martin-Eauclaire MF, Kharrat R, El Ayeb M, Darbon H, Rochat H, Crest M, and Sabatier J-M (2000) Maurotoxin and the Kv1.1 channel: voltage-dependent binding upon enantiomerization of the scorpion toxin disulfide bridge Cys31-Cys34. *J Pept Res* **55:**246–254.

Logsdon N, Kang J, Togo JA, Christian EP, and Aiyar J (1997) A novel gene, hKCa4, encodes the calcium-activated potassium channel in human T lymphocytes. *J Biol Chem* **272:**32723–32726.

Merrifield RB (1986) The solid phase peptide synthesis. *Science (Wash DC)* **232:**341–347.

Monaghan MM, Trimmer JS, and Rhodes KJ (2001) Experimental localization of Kv1 family voltage-gated K^+ channel alpha and beta subunits in rat hippocampal formation. *J Neurosci* **21:**5973–5983.

Pena TL and Rane SG (1999) The fibroblast intermediate conductance K(Ca) channel, FIK, as a prototype for the cell growth regulatory function of the IK channel family. *J Membr Biol* **172:**249–257.

Perez-Cornejo P, Stampe P, and Begenisich T (1998) Proton probing of the charybdotoxin binding site of Shaker K^+ channels. *J Gen Physiol* **111:**441–450.

Rane SG (2000) The growth regulatory fibroblast IK channel is the prominent electrophysiological feature of rat prostatic cancer cells. *Biochem Biophys Res Commun* **269:**457–463.

Rauer H and Grissmer S (1996) Evidence for an internal phenylalkylamine action on the voltage-gated potassium channel Kv1.3. *Mol Pharmacol* **50:**1625–1634.

Rauer H, Lanigan MD, Pennington MW, Aiyar J, Ghanshani S, Cahalan MD, Norton RS, and Chandy KG (2000) Structure-guided transformation of charybdotoxin yields an analog that selectively targets Ca^{2+}-activated over voltage-gated K^+ channels. *J Biol Chem* **275:**1201–1208.

Schreiber G and Fersht AR (1995) Energetics of protein-protein interactions: anal-

ysis of the barnase-barstar interface by single mutations and double mutant cycles. *J Mol Biol* **248:**478–486.
Thompson J and Begenisich T (2000) Electrostatic interaction between charybdotoxin and a tetrameric mutant of Shaker K^+ channels. *Biophys J* **78:**2382–2391.
Tytgat J, Chandy KG, Garcia ML, Gutman GA, Martin-Eauclaire MF, van der Walt JJ, and Possani LD (1999) A unified nomenclature for short-chain peptides isolated from scorpion venoms: alpha-KTx molecular subfamilies. *Trends Pharmacol Sci* **20:**444–447.
Vandorpe DH, Shmukler BE, Jiang L, Lim B, Maylie J, Adelman JP, Franceschi L, Cappellini MD, Brugnara C, and Alper SL (1998) cDNA cloning and functional characterization of the mouse Ca^{2+}-gated K^+ channel, mIK1. *J Biol Chem* **273:**21542–21553.
Visan V, Sabatier JM, and Grissmer S (2004) Block of maurotoxin and charybdotoxin on human intermediate-conductance calcium-activated potassium channels (hIKCa1). *Toxicon* **43:**973–980.
Wrisch A and Grissmer S (2000) Structural differences of bacterial and mammalian K^+ channels. *J Biol Chem* **275:**39345–39353.
Wulff H, Miller MJ, Hansel W, Grissmer S, Cahalan MD, and Chandy KG (2000) Design of a potent and selective inhibitor of the intermediate-conductance Ca^{2+}-activated K^+ channel, IKCa1: a potential immunosuppressant. *Proc Natl Acad Sci USA* **97:**8151–8156.

Address correspondence to: Prof. Dr. Stephan Grissmer, Department of Applied Physiology, University of Ulm, Albert-Einstein-Allee 11, D-89081 Ulm, Germany. E-mail: stephan.grissmer@medizin.uni-ulm.de